Single scattering turbulence model based on the division of effective scattering volume for ultraviolet communication

Tao Shan (山 涛)[1,2], Jianshe Ma (马建设)[1], Tianfeng Wu (吴天峰)[1], Zanqiu Shen (沈赞秋)[1,2], and Ping Su (苏 萍)[1,*]

[1]*Tsinghua Shenzhen International Graduate School, Tsinghua University, Shenzhen 518055, China*
[2]*Department of Precision Instrument, Tsinghua University, Beijing 100084, China*
**Corresponding author: su.ping@sz.tsinghua.edu.cn*

Received February 7, 2020; accepted September 4, 2020; posted online October 23, 2020

In this Letter, a single scattering turbulence model in a narrow beam case for ultraviolet (UV) communication is proposed based on the division of the effective scattering volume. This model takes the variation of atmospheric scattering, absorption, and turbulence in different paths into account. Meanwhile, the applicable transceiver configurations of this model are provided by analyzing path loss error caused by the single scattering assumption in the UV channel. Furthermore, we investigate the effect of turbulence on the probability density function of the arriving power in both coplanar and non-coplanar scenarios. The averaging effect of multipath propagation on the arriving power's fluctuations is presented. Then, the bit-error-rate performance is also studied. This work provides an efficient way for UV turbulence channel estimation.

Keywords: ultraviolet communication; single scattering; approximate model; atmospheric turbulence.
doi: 10.3788/COL202018.120602.

With the recent advances of ultraviolet (UV) sources and detectors in the solar-blind wavelength band, UV communication has attracted more attention for its potential advantages. The channel modeling of UV communication is of great significance in the research of UV communication[1–3]. In the past few decades, various UV communication channel models have been proposed, e.g., the single scattering models[4–6] and the multiple scattering models[7–9]. However, these models are confined to non-turbulent conditions. With the extension of the communication range, atmospheric turbulence leads to an unneglectable error with the effect of irradiance fluctuation and scintillation attenuation[10]. To improve accuracy, UV communication channel models are modified by applying the atmospheric turbulence theory. Some single scattering turbulence models have been derived by assuming that the channel characteristics of scattering, absorbing, and turbulence are constant in the whole effective scattering volume[11–13]. Moreover, the multiple scattering turbulence models have been developed, in which the effect of turbulence on each photon's path is considered[14,15]. However, the exploitation of UV communication availability in terms of geometrical configurations and atmospheric conditions is still needed[16].

In this Letter, we derive a single scattering turbulence model in a narrow beam case by dividing the effective scattering volume. Each sub-volume is approximated as a layer of the spherical crown (SC)[6]. In the case of weak or moderate optical turbulence, the arriving power through each sub-volume can be considered as a lognormal random variable and be obtained using the turbulence model in Ref. [13]. The probability distribution of the total arriving power can be obtained by summing these lognormal random variables up with the aid of the Wilkinson's method[17,18]. Since the transceiver configuration affects the path loss error, which is caused by approximating the actual arriving power with the single scattering power, we analyze the applicable transceiver configuration by simulating the proportion of the single scattering power in the total power. Based on this applicable configuration, we present the probability distribution of the arriving power in both coplanar and non-coplanar scenarios. Furthermore, the bit-error-rate (BER) performance is studied. Compared with the existing single scattering turbulence models[11–13], the proposed model is more effective. This is because the proposed model considers the variance of UV propagation characteristics in different paths. The averaging effect of the multipath propagation on the arriving power's fluctuations is presented. The effect of the non-coplanar scenario on the UV channel is also analyzed. In addition, the method of the transceiver configuration analysis prevents the path loss error of the single scattering model from being overestimated. Compared with the Monte-Carlo turbulence models[14,15], the proposed model requires much less calculation time. In the following, a detailed derivation of the proposed turbulence model is presented.

Figure 1 shows a typical non-line-of-sight (NLOS) UV communication geometry, in which the effective single scattering volume refers to the common volume intersected by the transmitted beam and the field of view (FOV). The distance from the transmitter (T) to the receiver (R), i.e., the communication range, is r. As in Ref. [6], the common volume is divided into N sub-volumes, each of

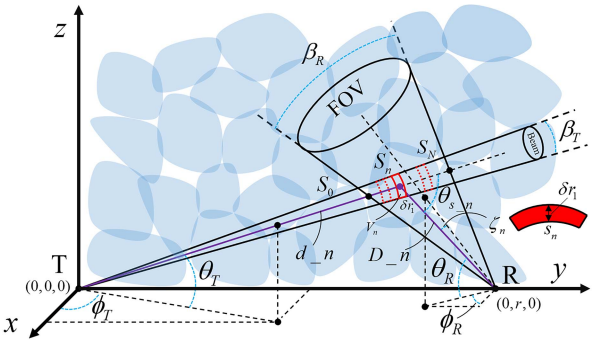

Fig. 1. Single scattering turbulence model geometry.

which can be approximated by an SC layer. The distances of the scattering point S_n in the nth sub-volume to T and R are d_n and D_n, respectively. $(\theta_T, \varphi_T, \beta_T)$ and $(\theta_R, \varphi_R, \beta_R)$ are the elevation angle, azimuth angel, and cone aperture of the transmitted beam or the FOV, respectively. θ_{s_n} denotes the angle between the arbitrary photon forward direction and the observation direction. ζ_n is the angle between the direction of R and the vector from R to S_n.

In the case of longer range communication, when using the SC model in Ref. [6] to estimate channel performance, the estimation error caused by ignoring turbulence effects will be larger. This is because the turbulence-induced scintillation reduces the UV communication performance in two aspects: scintillation attenuations and the arriving power fluctuation.

According to the Rytov approximation in Ref. [10], the scintillation attenuation induced by turbulence in a line-of-sight (LOS) link is defined as

$$\alpha_l = 2 \cdot \sqrt{23.17 C_n^2 (2\pi/\lambda)^{7/6} l^{11/6}}, \tag{1}$$

where C_n^2 denotes the refractive-index structure parameter, which is a measure of the strength of the atmospheric turbulence. On the whole, the value of C_n^2 ranges from 10^{-13} $\mathrm{m}^{-2/3}$ for strong turbulence to 10^{-17} $\mathrm{m}^{-2/3}$ for weak turbulence, with the value of 10^{-15} $\mathrm{m}^{-2/3}$ for moderate turbulence. l is the LOS communication distance, and λ is the wavelength. The variance of the log amplitude fluctuation in an LOS link for a plane wave is defined as follows:

$$\sigma_l^2 = 1.23 C_n^2 (2\pi/\lambda)^{7/6} l^{11/6}. \tag{2}$$

The NLOS communication links in a single scattering model can be split into two LOS paths[11]: one path is from the T to an effective scattering volume with the distance d_n, and the other path is from an effective scattering volume to R with the distance D_n.

In our model, the NLOS propagation paths through different sub-volumes lead to different turbulence-induced scintillation, i.e., attenuation α_l and variance σ_l^2. In the case of weak or moderate turbulence, the lognormal probability density function (PDF) of NLOS optical power through arbitrary sub-volume arriving at R is[13]

$$f(p_{r\_n}) = \frac{1}{\sqrt{2\pi}\sigma_{r\_n} p_{r\_n}} \exp\left\{ -\frac{\left[\ln\left(\frac{p_{r\_n}}{P_{\mathrm{NLOS}\_n}}\right) + \mu_{r\_n}\right]^2}{2\sigma_{r\_n}^2} \right\}, \tag{3a}$$

with

$$\sigma_{r\_n}^2 = \sigma_{d\_n}^2 + \sigma_{D\_n}^2, \tag{3b}$$

$$\mu_{r\_n} = \frac{\sigma_{d\_n}^2}{2} + \frac{\alpha_{d\_n} \cdot \ln 10}{10} + \frac{\sigma_{D\_n}^2}{2} + \frac{\alpha_{D\_n} \cdot \ln 10}{10}, \tag{3c}$$

where p_{r_n} denotes the possible value of arriving power P_{r_n} arriving at R through the nth sub-volume; $(\alpha_{d\_n}, \alpha_{D\_n})$ and $(\sigma_{d\_n}^2, \sigma_{D\_n}^2)$ can be calculated by Eqs. (1) and (2), respectively. P_{NLOS_n} refers to the arriving power through the nth sub-volume, while turbulence effects are ignored. P_{NLOS_n} can be calculated according to Eqs. (4.1)–(14) in Ref. [6]. Therefore, the arriving power P_{r_n} at R through the nth sub-volume is actually a continuous random variable in lognormal distribution. For simplicity, we assume that the arriving powers $P_{r\_1}, P_{r\_2}, \ldots, P_{r\_N}$ at R through different sub-volumes are independent, but not identically distributed because of the different distribution parameters in Eq. (3a). Thus, the total received power is a continuous random variable P_r, which is the sum of lognormal random variables of $P_{r\_1}, P_{r\_2}, \ldots, P_{r\_N}$. $N = 1$ means that the proposed model is transformed into the existing model, in which the propagation characteristics are assumed to be constant.

The lognormal sum distribution can be well approximated by another lognormal random variable[19], i.e.,

$$P_r = \sum_{n=1}^{N} P_{r\_n} = e^{X_1} + e^{X_2} + \ldots + e^{X_N} \approx e^{Z}, \tag{4}$$

where the random variables X_i and Z exhibit normal distributions associated with the lognormal random variables P_{r_n} and P_r, respectively. Wilkinson's method[17,18] suggests that the mean and variance of Z can be obtained by matching the first and second moments in both sides of Eq. (4). The kth moment of a lognormal random variable L with mean of logarithmic values μ and standard deviation of logarithmic values σ is expressed by $E[L^k] = \exp(k\mu + k^2\sigma^2/2)$, where $E[\,\cdot\,]$ denotes the expected value of the random variable. After some algebraic manipulations, we yield

$$\sigma_Z^2 = \ln(u_2/u_1^2 + 1), \tag{5a}$$

$$\mu_Z = \ln u_1 - \sigma_Z^2/2, \tag{5b}$$

where

$$u_1 = \sum_{i=1}^{N} e^{\mu_{X_i} + \frac{1}{2}\sigma_{X_i}^2}, \tag{5c}$$

$$u_2 = \sum_{i=1}^{N} e^{2\mu_{X_i} + \sigma_{X_i}^2} (e^{\sigma_{X_i}^2} - 1). \tag{5d}$$

Thus, the PDF of the total received power P_r with log-normal distribution is written as

$$f(p_r) = \frac{1}{\sqrt{2\pi}\sigma_Z p_r} \exp\left[-\frac{(\ln p_r - \mu_Z)^2}{2\sigma_Z^2}\right], \tag{6}$$

where p_r is the possible value of arriving total power P_r.

Based on the probability distribution of the received power P_r, the mean signal-to-noise ratio (SNR) in the case of a shot-noise-limited system under on–off keying, and direct detection is given by[10]

$$E[\mathrm{SNR}] = \frac{\mathrm{SNR}_0}{\sqrt{\frac{P_{r\_0}}{E[P_r]} + \mathrm{SNR}_0^2[\exp(\sigma_Z^2) - 1]}}, \tag{7}$$

where $P_{r\_0} = \sum P_{\mathrm{NLOS}\_n}$ is the total arriving power in the absence of turbulence, $\mathrm{SNR}_0 = [\eta_r P_{r\_0}/(2\,h\nu B)]^{-1/2}$ is the received SNR without turbulence, h is a Planck constant, ν is the optical frequency, B is the bandwidth, and η_r is the detector's quantum efficiency.

Accordingly, in the case of turbulence, the probability of error can be considered as the conditional probability, averaged over the PDF of the possible arriving power. The BER in turbulence is expressed as

$$E[\mathrm{BER}] = \frac{1}{2}\int_0^\infty f(p_r)\mathrm{erfc}\left(\frac{E[\mathrm{SNR}]}{2\sqrt{2}} \cdot \frac{p_r}{E[P_r]}\right)\mathrm{d}p_r, \tag{8}$$

where $\mathrm{erfc}(\cdot)$ denotes the complementary error function.

The results are shown in two parts. First, to obtain the applicable transceiver configuration of the single scattering turbulence model, we simulate the approximation path loss error caused by approximating the total arriving power with the single scattering power. Then, based on the applicable configuration analysis, we calculate the path loss, the distribution of the arriving power, and the BER performance using the proposed model. Unless otherwise specified, the parameters are assumed as follows: $P_t = 30\,\mathrm{mW}$, $A_r = 1.77\,\mathrm{cm}^2$, $\lambda = 260\,\mathrm{nm}$,$(\varphi_T, \varphi_R) = (90°, -90°)$, $\gamma = 0.017$, $g = 0.72$, $f = 0.5$, $(k_a, k_s^{\mathrm{Ray}}, k_s^{\mathrm{Mie}}) = (0.802, 0.266, 0.284)\ \mathrm{km}^{-1}$, which were used in the simulation analysis[6] and validated by the experiment measurement[5].

We first analyze the applicable transceiver configurations for the single scattering model by simulating the approximation path loss error when the single scattering power is used to estimate the total power. The approximation error err in decibels (dB) is defined as

$$\mathrm{err} = 10\log_{10}(P_{\mathrm{total}}/P_{\mathrm{single}}), \tag{9}$$

where P_{total} and P_{single} are the mean values of the arriving total power and the arriving single scattering power. P_{total} and P_{single} can be simulated by the Monte-Carlo model[15]. We assume the arriving total power is equal to the summation of the scattering powers of the first four scattering orders. To ensure that the beam is wrapped by FOV, and FOV is above the ground, so as to reduce the error of the SC model[6], we set (β_T, θ_R) to $(5°, 45°)$.

Figure 2 shows the approximation error err under different r and θ_T with $C_n^2 = 10^{-15}\ \mathrm{m}^{-2/3}$. Note that err increases as r or θ_T increases. That is because both the longer communication range and larger elevation angle require longer free paths for single scattering, which is in lower probability in the UV photon's propagation. In addition, the larger T elevation angle also causes the larger scattering angle, which means fewer UV photons can arrive at R by single scattering. The approximation error under different r and β_R is shown in Fig. 3, with $C_n^2 = 10^{-15}\ \mathrm{m}^{-2/3}$. With β_R increasing from 25° to 85°, the err first increases to the maximum and then decreases slightly. The minimal err appears when β_R is at the minimum. In general, the FOV angles have small impact on the approximation error (i.e., the proportion). But, a larger FOV captures more energy[6]. The absolute difference between the predicted arriving power by the single scattering model and the actual arriving power is more significant.

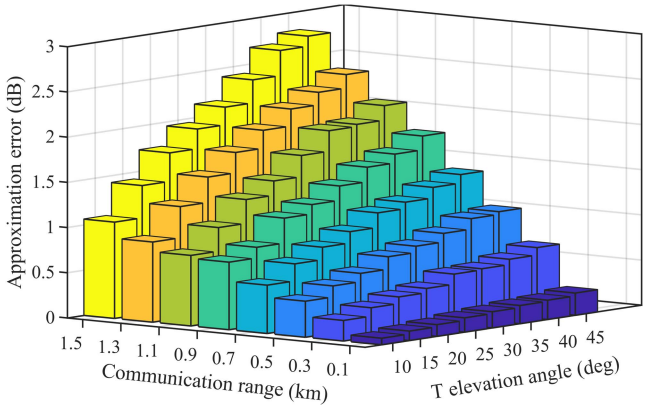

Fig. 2. Approximation error versus communication range and transmitter (T) elevation angle ($\beta_T = 5°$, $\theta_R = 45°$, $\beta_R = 65°$).

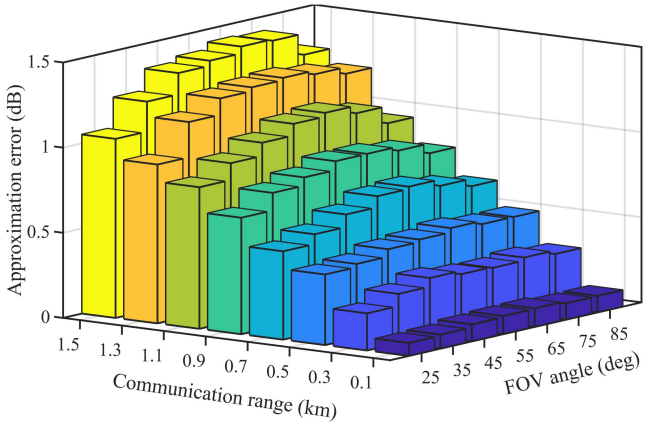

Fig. 3. Approximation error versus communication range and R FOV angle ($\beta_T = 5°$, $\theta_T = 15°$, $\theta_R = 45°$).

Based on the impacts of transceiver configuration on the approximation error, we can select a lower T elevation angle or a smaller R FOV angle to reduce the approximation error in the single scattering model. The effective range of the single scattering model can be enlarged by reducing the T elevation angle or the FOV angle. Thus, we can employ the single scattering turbulence model to analyze the characteristics of long distance turbulent channels. This transceiver configuration analysis can also be used to keep the single scattering model valid in various scenarios. Based on the derivation of the proposed model and applicable configuration analysis mentioned above, $(\beta_T, \theta_T, \beta_R, \theta_R)$ is set to $(5°, 15°, 25°, 45°)$.

The impacts of atmospheric turbulence on UV communication are shown in Figs. 4– 7. The variation of path loss under different turbulence strengths is shown in the Fig. 4, where C_n^2 ranges from 10^{-17} $\mathrm{m}^{-2/3}$ to 10^{-15} $\mathrm{m}^{-2/3}$. Calculation results indicate that the turbulence-induced attenuation increases as the transmission distance increases or as the value of C_n^2 increases. The turbulence effect is negligible in a short distance (100 m) communication and in the case of weak turbulence, but not in a long distance (1000 m) communication or in the case of moderate turbulence.

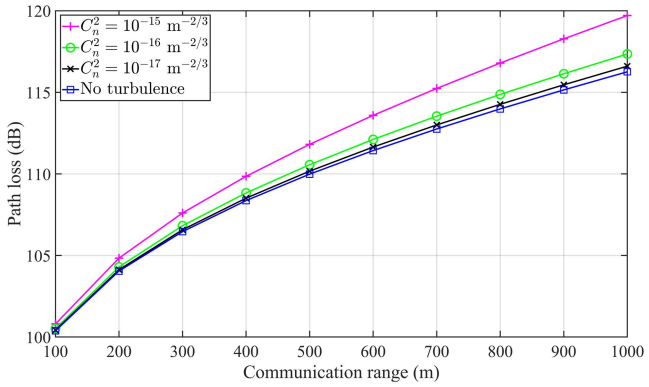

Fig. 4. Path loss under different turbulence conditions.

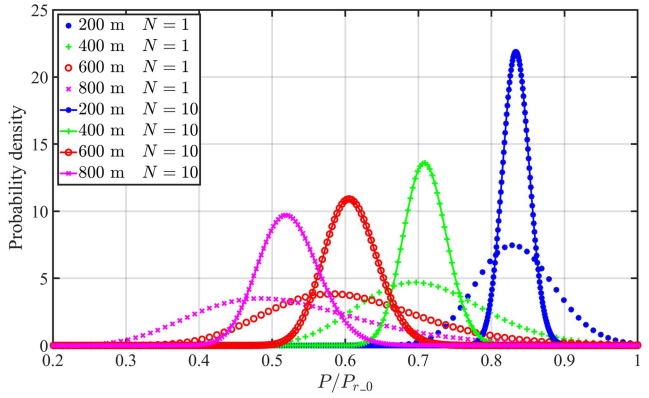

Fig. 5. PDF of the normalized arriving power under different communication ranges and different N values.

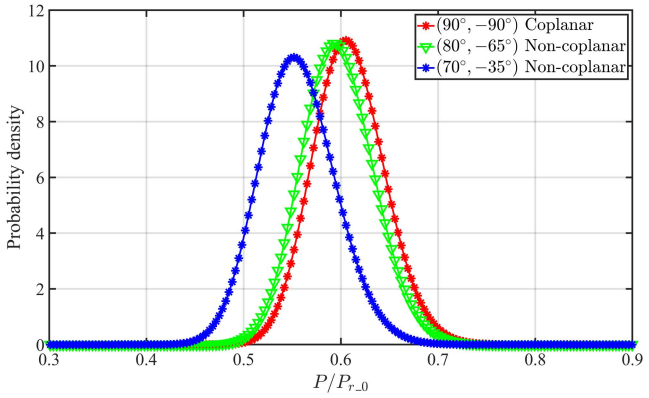

Fig. 6. PDF of the normalized arriving optical power in non-coplanar geometry.

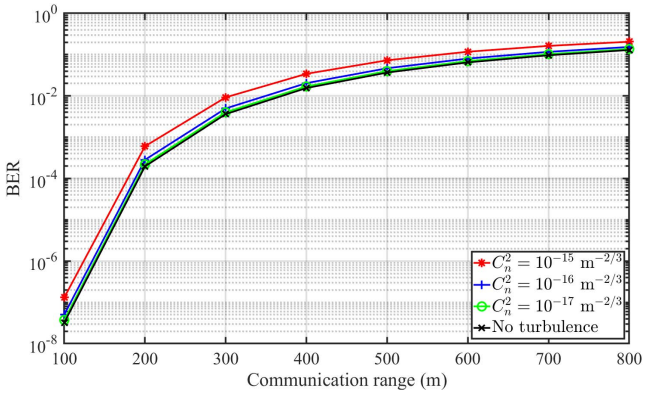

Fig. 7. BER versus UV communication range r.

Figure 5 shows the distribution of the arriving power under different communication ranges and different numbers of the sub-volume with $C_n^2 = 10^{-15}$ $\mathrm{m}^{-2/3}$. As shown in Fig. 5, the variance of the arriving power distribution keeps increasing, and the mean keeps decreasing, as the communication range increases. Furthermore, we utilize N to distinguish whether the variations of atmospheric characteristics in the scattering volume are taken into account. Based on the analysis in Ref. [18], without loss of generality, we assume that $N = 10$ corresponds to the proposed model, in which the variation of atmospheric scattering, absorption, and turbulence is in different paths. $N = 1$ corresponds to the existing models, in which the propagation characteristics are assumed constant in the whole system[11–13]. The variance of $N = 10$ is smaller than the variance of $N = 1$. The mean of logarithmic values, i.e., μ_Z in Eq. (7), remains unchanged. The mean of the arriving power when $N = 10$ is greater than the mean when $N = 1$. Figure 5 shows that the arriving power from different paths can mitigate the turbulence effect on the arriving total power[14]. The existing single scattering turbulence model and the proposed one both require the narrow beam case. Because β_R is larger than β_T, the effective scattering volume is almost an elongated cylinder. UV photons can arrive at the R through different paths.

The multipath propagation effect is significant. The effect of multipath propagation is considered in the proposed model, which indicates that the proposed model is more effective than the existing one. Apart from the proposed model, the effect of multipath propagation can only be simulated by the Monte-Carlo method[14,15], which requires more simulation time and computing resources than the proposed model.

Compared with the existing models, the proposed model is not limited in coplanar geometry. In the non-coplanar case, the distribution of the arriving power is illustrated in Fig. 6 with various pairs of the T/R's azimuth angle (φ_T, φ_R). The communication range r is set to 600 m. Without loss of generality, it is assumed that the effective scattering volume is in the first octant, in which φ_T ranges from 0° to 90°, and φ_R ranges from −90° to 0°. Compared with the parameters in the coplanar case, the variance is greater, and the mean is smaller in the non-coplanar case. The non-coplanar effect is more significant with φ_T decreasing or φ_R increasing. This is because the non-coplanar geometry implies a longer link than the coplanar one, which affects the value of turbulence parameters α_l and σ_l^2.

The impact of communication range on BER performance under different turbulence conditions is shown in Fig. 7. The following parameters are assumed: $B = 3\,\mathrm{kbit/s}$ and $\eta_r = 0.2$. It is suggested that more significant BER performance reduction occurs in stronger turbulence. When the communication range is 100 m (short distance), the effect of turbulence can be ignored under a weak or moderate turbulence condition. Figure 7 indicates that the BER will increase significantly in long-range UV communication and strong turbulence.

In summary, we propose a single scattering turbulence model, in which we consider the variation in the photons' propagation characteristics in different turbulent paths. The analysis of applicable transceiver configuration shows that the single scattering turbulence model is more valid in a lower elevation angle or smaller FOV scenario. Under the applicable single scattering configuration, we analyze the distribution of total arriving power in both the coplanar and non-coplanar case. The effect of multipath propagation is presented. Before the proposed model, only the Monte-Carlo model geometry takes the effect of multipath propagation and non-coplanar into account. However, the Monte-Carlo method is usually time-consuming. This work provides a more efficient solution for channel estimation in NLOS UV communication.

This work was supported by the Basic Research Program of Shenzhen (No. JCYJ20170412171744267)

References

1. R. Yuan and J. Ma, Chin. Commun. **13**, 63 (2016).
2. X. Zhou, J. Li, W. Lu, Y. Wang, X. Song, S. Yin, X Tan, Y. Lü, H. Guo, G. Gu, and Z. Feng, Chin. Opt. Lett. **16**, 060401 (2018).
3. X. Zhou, X. Tan, Y. Wang, X. Song, T. Han, J. Li, W. Lu, G. Gu, S. Liang, Y. Lü, and Z. Feng, Chin. Opt. Lett. **17**, 090401 (2019).
4. M. R. Luettgen, J. H. Shapiro, and D. M. Reilly, J. Opt. Soc. Am. A **8**, 1964 (1991).
5. Z. Xu, H. Ding, B. M. Sadler, and G. Chen, Opt. Lett. **33**, 1860 (2008).
6. T. Wu, J. Ma, R. Yuan, P. Su, and J. Cheng, IEEE Photon. Technol. Lett. **31**, 265 (2019).
7. H. Ding, G. Chen, A. K. Majumdar, B. M. Sadler, and Z. Xu, IEEE J. Sel. Areas Commun. **27**, 1535 (2009).
8. R. Yuan, J. Ma, P. Su, Y. Dong, and J. Cheng, IEEE Trans. Commun. **68**, 334 (2020).
9. R. Yuan, J. Ma, P. Su, and Z. He, IEEE Commun. Lett. **20**, 2366 (2016).
10. L. C. Andrews and R. L. Phillips, *Laser Beam Propagation through Random Media* (SPIE, 2005).
11. H. Ding, G. Chen, A. K. Majumdar, B. M. Sadler, and Z. Xu, Proc. SPIE **8038**, 80380J (2011).
12. Y. Zuo, J. Wu, H. Xiao, and J. Lin, Chin. Commun. **10**, 52 (2013).
13. M. H. Ardakani, A. R. Heidarpour, and M. Uysal, in *2015 4th International Workshop on Optical Wireless Communications (IWOW)* (2015), p. 55.
14. P. Wang and Z. Xu, Opt. Lett. **38**, 2773 (2013).
15. L. Liao, Z. Li, T. Lang, and G. Chen, Opt. Express **23**, 21825 (2015).
16. M. Uysal, C. Capsoni, Z. Ghassemlooy, A. Boucouvalas, and E. Udvary, eds., *Optical Wireless Communications: An Emerging Technology* (Springer, 2016).
17. S. C. Schwartz and Y. S. Yeh, Bell System Tech. J. **61**, 1441 (1982).
18. L. Fenton, IRE Trans. Commun. Syst. **8**, 57 (1960).
19. G. L. Stüber and G. L. Stèuber, *Principles of Mobile Communication* (Springer, 1996).